

This article was downloaded by: [National Chiao Tung University 國立交通大學]

On: 24 April 2014, At: 23:29

Publisher: Taylor & Francis

Informa Ltd Registered in England and Wales Registered Number: 1072954 Registered office: Mortimer House, 37-41 Mortimer Street, London W1T 3JH, UK



Mechanics Based Design of Structures and Machines: An International Journal

Publication details, including instructions for authors and subscription information:

<http://www.tandfonline.com/loi/lmbd20>

Outrigger Force Measure for Mobile Crane Safety Based on Linear Programming Optimization[#]

Shyr-Long Jeng^a, Chia-Feng Yang^b & Wei-Hua Chieng^b

^a Department of Automatic Engineering, Ta Hwa Institute of Technology, Qionglin Shiang Hsinchu County, Taiwan, Republic of China

^b Department of Mechanical Engineering, National Chiao Tung University, Hsinchu City, Taiwan, Republic of China

Published online: 21 May 2010.

To cite this article: Shyr-Long Jeng, Chia-Feng Yang & Wei-Hua Chieng (2010) Outrigger Force Measure for Mobile Crane Safety Based on Linear Programming Optimization[#], *Mechanics Based Design of Structures and Machines: An International Journal*, 38:2, 145-170, DOI: [10.1080/15397730903482702](https://doi.org/10.1080/15397730903482702)

To link to this article: <http://dx.doi.org/10.1080/15397730903482702>

PLEASE SCROLL DOWN FOR ARTICLE

Taylor & Francis makes every effort to ensure the accuracy of all the information (the "Content") contained in the publications on our platform. However, Taylor & Francis, our agents, and our licensors make no representations or warranties whatsoever as to the accuracy, completeness, or suitability for any purpose of the Content. Any opinions and views expressed in this publication are the opinions and views of the authors, and are not the views of or endorsed by Taylor & Francis. The accuracy of the Content should not be relied upon and should be independently verified with primary sources of information. Taylor and Francis shall not be liable for any losses, actions, claims, proceedings, demands, costs, expenses, damages, and other liabilities whatsoever or howsoever caused arising directly or indirectly in connection with, in relation to or arising out of the use of the Content.

This article may be used for research, teaching, and private study purposes. Any substantial or systematic reproduction, redistribution, reselling, loan, sub-licensing, systematic supply, or distribution in any form to anyone is expressly forbidden. Terms & Conditions of access and use can be found at <http://www.tandfonline.com/page/terms-and-conditions>

OUTRIGGER FORCE MEASURE FOR MOBILE CRANE SAFETY BASED ON LINEAR PROGRAMMING OPTIMIZATION[#]

Shyr-Long Jeng,¹ Chia-Feng Yang,² and Wei-Hua Chieng²

¹Department of Automatic Engineering, Ta Hwa Institute of Technology, Qionglin Shiang Hsinchu County, Taiwan, Republic of China

²Department of Mechanical Engineering, National Chiao Tung University, Hsinchu City, Taiwan, Republic of China

This work presents a linear programming simplex method for evaluating allowable reaction forces of multiple outriggers with stability constraints. Minimum/maximum pruning approach is adopted to increase the computational efficiency of assessing the outrigger forces when a mobile crane is kept level by the supports of four outriggers. Determining the outrigger forces is an effective means of preventing a mobile crane from tipping over or outrigger failures. Two indices, i.e., moment-index and force-index, which quantify the tendency of tip-over behavior of mobile cranes and examine the bearing capacity of outrigger, are introduced to improve the safety measures. The safety hoist criteria of two mobile crane types equipped with different outriggers are analyzed to demonstrate the feasibility of the proposed scheme. An intelligent anti-upset device that utilizes the outrigger-based stability measures and selectively suppresses critical steering commands in real time is implemented to ensure safe crane operations.

Keywords: Linear programming; Mobile crane; Overturning stability.

INTRODUCTION

Mobile crane stability is an extremely important safety issue. Failure to maintain stability is associated with serious accidents that can injure operators or damage equipment. Mobile crane accidents depend on a number of factors, including poor ground conditions, failure to use or fully extend outriggers or stabilizers, failure to level the crane, rapid slewing, and high-wind conditions. Statistics (Neitzel et al., 2001) show that at least 50% of crane accidents occur because mobile cranes or outriggers are not operated properly.

Some investigations have quantified overturning stability of mobile vehicles or slow-moving legged machines. McGhee and Frank (1968) developed a static stability margin for an arbitrary support base, which is equal to the shortest distance from the vertical projection of the gravity center to any point on the support

Received June 4, 2008; Accepted October 10, 2008

[#]Communicated by S. Azarm.

Correspondence: Shyr-Long Jeng, Department of Automatic Engineering, Ta Hwa Institute of Technology, No. 1, Dahua Road, Qionglin Shiang Hsinchu County, Taiwan 30740, Republic of China; E-mail: aetstl@thit.edu.tw

base boundary. Mezzuri and Klein (1985) extended the stability margin to account for the effects of rough terrain when moving a base manipulator. A quantitative measure, termed the energy stability margin, is confined to the stability analysis of vehicles that are subject to gravity. Nagy et al. (1994) and Ghasempoor and Sepehri (1998) utilized the energy-based stability measures on the locomotion of multi-legged robot or heavy-duty manipulator machines, respectively. Sugano et al. (1993) developed zero-moment criterions to distinguish the stability in controlling mobile manipulator. Lim et al. (2004) employed zero-moment point theory to analyze the tip-over stability for a hydraulic excavator. Papadopoulos and Rey (2000) presented the force-angle stability margin measure operating over uneven terrain. These stability measures have typically assumed that the manipulator stands on solid ground. Although the overturning stability of the crane has received considerable attention, the extent to which ground conditions or outrigger legs collapsed has not been addressed.

Tamate et al. (2005) examined a serial of experimental analysis to investigate the influence of outriggers penetrating the ground on mobile crane stability. Kato and Ito (1980), who analyzed the static stability of a crane carrier, proposed a theoretical formula that explains the elastic deformation of carriers. Dubowsky et al. (1991) developed an analysis method of dynamic spatial behavior by considering the flexibility of the manipulators. Mijailovic and Selmic (2004), Aslan et al. (1999), and Towarek (1998) examined angular ball bearing deformation, flexible booms, and soil, respectively. Abo-Shanab and Sepehri (2005) demonstrated manipulator movements, the contact between the base and ground, hydraulic compliance, and frictional properties between wheels and ground on tip-over stability of heavy-duty hydraulic log-loader machines. These studies (Abo-Shanab and Sepehri, 2005; Aslan et al., 1999; Dubowsky et al., 1991; Kato and Ito, 1980; Mijailovic and Selmic, 2004; Towarek, 1998) described the combined vehicle suspension-ground-outrigger by using the spring-damping model, which is appropriate for off-line analysis. Ground conditions can vary dramatically from one workplace to another, and even within the same workplace. Soils range from wet sand that can only support 2,000 pounds per square foot to dry hard clay that can support 4,000 pounds per square foot to a well-cemented hardpan that can support as much as 10,000 pounds per square foot. In the workplace, accurately obtaining the coefficients of spring and damping is rather difficult. Evaluating the reaction forces while assuming that the ground conditions remain the same irregardless of location would be unreasonable.

Capable of determining lifted capacities of a crane by using load charts or mathematic equations calculated by the ratio of the overturning moment and stabilizing moment, conventional antiupset devices (Al-lami and Benazzouz, 1991; Neitzel et al., 2001; Queensland Government, 2006; Truninger, 1992) provide crane operators with a warning signal if the overturning moment required to upset the crane is approached or exceeded. Although the overturning stability of the crane has received considerable attention, outrigger forces-related information is missing except that the force sensors of the outrigger are provided. While Zhou et al. (2007) proposed a safety system that detects hydraulic outrigger forces by a force transducer, that system cannot accurately predict the lifted load, boom angles, and load radius based on the distributions of outrigger forces. Studying addition to evaluating the allowable reaction outrigger forces, this work accurately predicts the risk of overturning for a mobile crane. Real-time monitoring of outrigger capacities

provides crane operators with relevant information to perform hoist operations safely and efficiently.

MATHEMATICAL MODEL OF MOBILE CRANE

Figure 1 presents an appearance of a mobile hydraulic crane, which is set horizontally on plat ground. Taking the plat ground as the datum level, a rectangular coordinate with X-, Y-, and Z-axis is setup at the intersection with the rotational center axis. The following discrete components of the mobile crane are identified: the gravitational force of the lower machine is assumed as F_{weight} with the gravitational center at (x_{weight}, y_{weight}) ; the gravitational weight of a lifted load is F_{load} at position (x_{load}, y_{load}) ; the gravitational force of each section of the telescopic boom is F_{pbj} ($j = 1, \dots, m$) with the corresponding gravitational center at (x_{pbj}, y_{pbj}) ; the three components of reaction forces acting on each outrigger are $(R_{i,x}, R_{i,y}, R_{i,z})$ ($i = 1, \dots, n$), where n is the total number of outriggers; and, each outrigger position under the contact point is at (x_{Ri}, y_{Ri}) . $(F_{eq,x}, F_{eq,y}, F_{eq,z})$ and $(M_{eq,x}, M_{eq,y}, M_{eq,z})$ are the equilibrium force and moment due to centrifugal force, harmonic loads induced by rapid loading at the hook, and strong wind imposed on the rotational center. For a rigid body to be in equilibrium, the net force and net moment on the crane body must equal zero. This equilibrium condition can be represented using the following equations:

$$\sum F_x = F_{eq,x} + \sum_{i=1}^n R_{i,x} = 0, \tag{1.a}$$

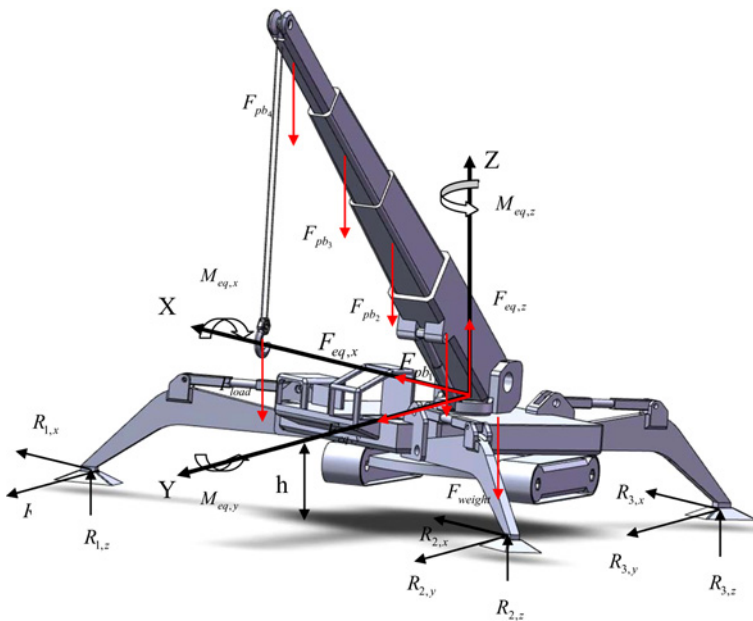


Figure 1 Mechanical model of a mobile crane.

$$\sum F_y = F_{\text{eq},y} + \sum_{i=1}^n R_{i,y} = 0, \quad (1.b)$$

$$\sum F_z = -F_{\text{load}} - F_{\text{weight}} - \sum_{j=1}^m F_{\text{pb}_j} + F_{\text{eq},z} + \sum_{i=1}^n F_{i,z} = 0, \quad (1.c)$$

$$\begin{aligned} \sum M_x = & -F_{\text{load}} \cdot y_{\text{load}} - F_{\text{weight}} \cdot y_{\text{weight}} - \sum_{j=1}^m F_{\text{pb}_j} \cdot y_{\text{pb}_j} \\ & + M_{\text{eq},x} + \sum_{i=1}^n R_{i,z} \cdot y_{R_i} + \sum_{i=1}^n R_{i,y} \cdot h = 0, \end{aligned} \quad (1.d)$$

$$\begin{aligned} \sum M_y = & F_{\text{load}} \cdot x_{\text{load}} + F_{\text{weight}} \cdot x_{\text{weight}} + \sum_{j=1}^m F_{\text{pb}_j} \cdot x_{\text{pb}_j} \\ & + M_{\text{eq},y} - \sum_{i=1}^n R_{i,z} \cdot x_{R_i} - \sum_{i=1}^n R_{i,x} \cdot h = 0, \end{aligned} \quad (1.e)$$

$$\sum M_z = M_{\text{eq},z} - \sum_{i=1}^n R_{i,x} \cdot y_{R_i} + \sum_{i=1}^n R_{i,y} \cdot x_{R_i} = 0, \quad (1.f)$$

where h is the height between the contact point and the rotational center. These equations, which can be rewritten with unknowns $R_{i,z}$ ($i = 1, \dots, n$) on the left side and given input variables on the right side, are solved for vertical reaction forces at each outrigger using matrix manipulation.

$$\begin{bmatrix} 1 & 1 & \cdots & 1 \\ x_{R_1} & x_{R_2} & \cdots & x_{R_n} \\ y_{R_1} & y_{R_2} & \cdots & y_{R_n} \end{bmatrix} \begin{bmatrix} R_{1,z} \\ R_{2,z} \\ \vdots \\ R_{n,z} \end{bmatrix} = \begin{bmatrix} F_{\text{all},z} \\ M_{\text{all},y} \\ M_{\text{all},z} \end{bmatrix}, \quad (2)$$

where

$$F_{\text{all},z} = F_{\text{load}} + F_{\text{weight}} - F_{\text{eq},z} + \sum_{j=1}^m F_{\text{pb}_j},$$

$$M_{\text{all},y} = F_{\text{load}} \cdot x_{\text{load}} + F_{\text{weight}} \cdot x_{\text{weight}} + \sum_{j=1}^m F_{\text{pb}_j} \cdot x_{\text{pb}_j} + M_{\text{eq},y} - F_{\text{eq},y} \cdot h,$$

$$M_{\text{all},x} = F_{\text{load}} \cdot y_{\text{load}} + F_{\text{weight}} \cdot y_{\text{weight}} + \sum_{j=1}^m F_{\text{pb}_j} \cdot y_{\text{pb}_j} - M_{\text{eq},x} + F_{\text{eq},x} \cdot h.$$

Outrigger Reaction Forces

Overtuning stability of a mobile crane determined using the outrigger forces is similar to the stability criterion defined based on ground condition. The outrigger force $R_{i,z}$ can be represented in such a way that its positive value corresponds to ground deflection. When the outrigger force $R_{i,z}$ is negative, support loss occurs. Overtuning stability can be established by determining whether the forces within a feasible region, are higher or lower than zero.

Lemma. *If outrigger forces with nonnegative values satisfy static equilibrium in (2), then the mobile crane is stable; otherwise, the mobile crane is unstable.*

When outriggers are operated at more than three positions, the static behavior of a mobile crane is an underdetermined linear system, for which number of static equations is less than unknown. Vertical reaction force $R_{i,z}$ cannot be determined directly using only the equilibrium equation in (2). At least one solution for reaction forces can satisfy the equilibrium equation when the underdetermined system is consistent with the stability constraints. Accessing allowable reaction forces of multiple outriggers requires evaluating all possible outrigger forces. Instead, a scheme assessing the allowable ranges of outrigger forces increases computational efficiency as described below.

Multiple Position Stabilizer Legs

A mobile crane is kept level using n outriggers, where n is greater than three. Rearranging the lasting terms of outrigger forces $R_{k,z}$, $k = 4, \dots, n$ into the right side of (2) converts a system of three equations with n unknowns into the following equivalent form:

$$\begin{bmatrix} 1 & 1 & 1 \\ x_{R_1} & x_{R_2} & x_{R_3} \\ y_{R_1} & y_{R_2} & y_{R_3} \end{bmatrix} \begin{bmatrix} R_{1,z} \\ R_{2,z} \\ R_{3,z} \end{bmatrix} = \begin{bmatrix} F_{\text{all},z} - \sum_{k=4}^n R_{k,z} \\ M_{\text{all},y} - \sum_{k=4}^n R_{k,z} \cdot x_{R_k} \\ M_{\text{all},x} - \sum_{k=4}^n R_{k,z} \cdot y_{R_k} \end{bmatrix}. \quad (3)$$

Using Cramer's rule, outrigger forces $R_{i,z}$ ($i = 1, 2, 3$) can be derived using determinants

$$\begin{bmatrix} R_{1,z} \\ R_{2,z} \\ R_{3,z} \end{bmatrix} = \begin{bmatrix} \frac{Q_1 - \sum_{k=4}^n R_{k,z} \cdot \Delta_{1,k}}{\Delta_{R_1 R_2 R_3}} \\ \frac{Q_2 - \sum_{k=4}^n R_{k,z} \cdot \Delta_{2,k}}{\Delta_{R_1 R_2 R_3}} \\ \frac{Q_3 - \sum_{k=4}^n R_{k,z} \cdot \Delta_{3,k}}{\Delta_{R_1 R_2 R_3}} \end{bmatrix}, \quad (4)$$

where

$$\begin{aligned} Q_i &= -M_{\text{all},y}(x_{R_{i+1}} - x_{R_{i+2}}) - M_{\text{all},x}(y_{R_{i+2}} - y_{R_{i+1}}) \\ &\quad - F_{\text{all},z}(x_{R_{i+2}} \cdot y_{R_{i+1}} - x_{R_{i+1}} \cdot y_{R_{i+2}}), \\ \Delta_{1,k} &= \Delta_{R_k R_2 R_3}, \\ \Delta_{2,k} &= \Delta_{R_1 R_k R_3}, \\ \Delta_{3,k} &= \Delta_{R_1 R_2 R_k}, \\ \Delta_{R_i R_j R_k} &= \begin{vmatrix} 1 & 1 & 1 \\ x_{R_i} & x_{R_j} & x_{R_k} \\ y_{R_i} & y_{R_j} & y_{R_k} \end{vmatrix}. \end{aligned}$$

To stop a crane from turning over, outrigger forces must be greater than or equal to zero. These constraints on outrigger force variables can be rewritten as

$$\frac{Q_i - \sum_{k=4}^n R_{k,z} \cdot \Delta_{i,k}}{\Delta_{R_1 R_2 R_3}} \geq 0 \quad \text{for } i = 1, 2, 3; \quad (5.a)$$

$$R_{k,z} \geq 0 \quad \text{for } k = 4, \dots, n \quad (5.b)$$

The outrigger forces, $R_{i,z}$, $i = 1, \dots, n$, are chosen as the design variables whose value can be randomly selected from the inequality constraint set in (5). If the constraint set is found to be feasible, the lower and upper bounds of each outrigger force may be obtained. When the set of feasible solutions is empty, the outrigger forces fail to satisfy the constraint set and make the crane overturning. The problem of obtaining the lower limit of outrigger forces $R_{i,z}$ can be formulated by considering the outrigger forces $R_{i,z}$ as the objective function. The design objective is to minimize the outrigger force $R_{i,z}$ and, simultaneously, satisfy the inequality constraint set. Similarly, no restriction, such as upper limit of the outrigger force $R_{i,z}$, is the same as maximization of the outrigger force. The formulation has n design variables and n inequality constraints. A set of $2 \cdot n$ independent objective functions is utilized to derive the smallest and largest allowable values for each outrigger force $R_{i,z}$. The optimum problem, including multiple linear objective functions and linear constraint functions, is a linear programming problem. The optimum solution for a linear programming problem always resides on the boundary of a feasible region. The two-phase simplex algorithm (Siddall, 1972) is applied to find the lower and upper bounds of each outrigger force.

Four-Point Outrigger System

Consider a mobile crane is generally setup using four outriggers, each located at a corner. The procedure to determine the available ranges of the outrigger forces can be simplified by using a minimum/maximum operation discussed below. According to (4), the unknown variables $R_{1,z}$, $R_{2,z}$, and $R_{3,z}$ can be expressed as follows:

$$\begin{bmatrix} R_{1,z} \\ R_{2,z} \\ R_{3,z} \end{bmatrix} = \begin{bmatrix} \frac{Q_1 - R_{4,z} \cdot \Delta_{1,4}}{\Delta_{R_1 R_2 R_3}} \\ \frac{Q_2 - R_{4,z} \cdot \Delta_{2,4}}{\Delta_{R_1 R_2 R_3}} \\ \frac{Q_3 - R_{4,z} \cdot \Delta_{3,4}}{\Delta_{R_1 R_2 R_3}} \end{bmatrix}. \quad (6)$$

The fundamental geometric meaning of the absolute value of $\Delta_{R_i R_j R_k}$ is equal to the area of a triangular formed by supporting outriggers R_i , R_j , and R_k . According to Lemma, all outrigger forces $R_{i,z}$ should be nonnegative for a stable solution of a mobile crane. That is, constraints on outrigger force $R_{i,z}$, $i = 1, 2$, and 3 can be

rewritten as the following inequalities:

$$\begin{cases} \frac{Q_1 - R_{4,z} \cdot \Delta_{1,4}}{\Delta_{R_1 R_2 R_3}} \geq 0 \\ \frac{Q_2 - R_{4,z} \cdot \Delta_{2,4}}{\Delta_{R_1 R_2 R_3}} \geq 0 \\ \frac{Q_3 - R_{4,z} \cdot \Delta_{3,4}}{\Delta_{R_1 R_2 R_3}} \geq 0 \end{cases} \quad (7)$$

The constraints are represented by inequalities, each related to a feasible range of static stability, yielding lower and upper bounds of outrigger forces.

Notably, inequality of $R_{4,z} \geq 0$ yields outrigger force variable $R_{4,z}$, including a lower bound value of zero. To establish an arbitrary starting algorithm, this study may initiate the upper and lower bounds of outrigger force of $R_{4,z}$ into ∞ and 0, respectively. When the value for $\Delta_{1,4}/\Delta_{R_1 R_2 R_3}$ is positive, the inequality of (7) becomes

$$R_{4,z} \leq \frac{Q_1}{\Delta_{1,4}} \quad (8)$$

A new upper bound of outrigger force $R_{4,z}$, denoted by $R_{4,max}$, must be restricted by using the minimum operation

$$R_{4,max} = \min \left(R_{4,max}, \frac{Q_1}{\Delta_{1,4}} \right) \quad (9)$$

Similarly, the lower bound for outrigger force $R_{4,z}$, denoted by $R_{4,min}$, may be pruned the retrieval region for the case when $\Delta_{1,4}/\Delta_{R_1 R_2 R_3}$ is a negative number.

$$R_{4,min} = \max \left(R_{4,min}, \frac{Q_1}{\Delta_{1,4}} \right) \quad (10)$$

Different values of $\Delta_{1,4}/\Delta_{R_1 R_2 R_3}$ yield rigorous upper and lower limits on the outrigger force value, $R_{4,z}$. The procedure reduces two bounds until available states satisfy the set of inequalities constraints in (7). The lower bound of outrigger force $R_{4,z}$ must be less than or equal to the upper bound of outrigger force $R_{4,z}$. If the feasible region of outrigger force $R_{4,z}$ is null, then no solution satisfies the static equilibrium and the mobile crane is unstable. This minimum/maximum procedure determines the overturning stability as listed in the Appendix.

Moment and Force Indices

The stabilizing moment, which typically keeps the crane upright, can be expressed as follows (Fig. 2):

$$M_{stabilize} = F_{weight} \cdot d_{weight} \quad (11)$$

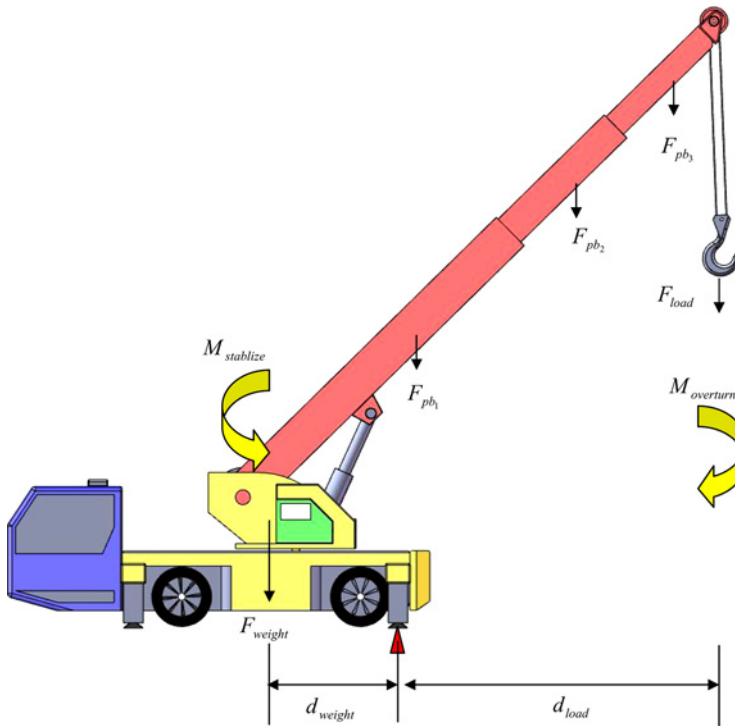


Figure 2 The stabilized and overturning moments.

and the overturning moment, which generally tips the crane over, is

$$M_{\text{overturn}} = F_{\text{load}} \cdot d_{\text{load}} + \sum_{i=1}^n F_{\text{pb}_i} \cdot d_{\text{pb}_i}, \quad (12)$$

where d_{weight} , d_{load} , and d_{pb_i} are the perpendicular distances between the overturning edge connected by the rear two outriggers and projection points F_{weight} , F_{load} , and F_{pb_i} forces, respectively. The tipping load, $F_{\text{load,tip}}$, is a critical load lifted, in which the overturning moment M_{overturn} is equal to stabilizing moment $M_{\text{stabilize}}$, i.e.,

$$F_{\text{load,tip}} = \frac{F_{\text{weight}} \cdot d_{\text{weight}} - \sum_{i=1}^n F_{\text{pb}_i} \cdot d_{\text{pb}_i}}{d_{\text{load}}}. \quad (13)$$

The maximum bearing capacity R_{crit} between outrigger and ground can be determined by the maximum axial load of the outrigger provided by the crane's manufacturer, or the resistant strength of the current ground type. Two relative stability indices for risk evaluation of instability of a mobile crane are defined as follows:

$$S_{\text{moment}} = \frac{F_{\text{load}}}{F_{\text{load,tip}}} \quad (14)$$

and

$$S_{\text{force}} = \frac{\max(R_{1z,\text{max}}, R_{2z,\text{max}}, \dots, R_{nz,\text{max}})}{R_{\text{crit}}} \quad (15)$$

The moment index S_{moment} , which is the ratio of current load lifted to tipping load, is utilized to measure overturning tendency. When the current load lifted is less than the tipping load, i.e., the S_{moment} index is less than unity, the stabilizing moment $M_{\text{stabilize}}$ provides a sufficient moment to prevent overturning. Conversely, when the load lifted increases close to the tipping load, the stabilizing moment $M_{\text{stabilize}}$ resisting overturning becomes gradually inadequate such that the margin against failure decreases for the entire machine. The force index S_{force} is the ratio of maximum allowed outrigger forces to the outrigger limit R_{crit} . When the maximum outrigger force exceeds the mechanical limit or the ground strength, outrigger legs may become cracked. As these two indices increase, the stability of the crane decreases.

CASE EXAMPLES

Example 1: Mobile Rotary Crane with Four Outriggers

An 18-ton hydraulic mobile crane has a telescopic boom consisting of four segments (Fig. 3). Maximum boom length is 30.6m and the rigid boom weighs approximately 2.8 tons. Each outrigger is extended to 2.1m outwardly. Dynamic effects are neglected by assuming that the mobile crane operates at a slow speed. Table 1 lists the basic numerical data for the mobile crane.

The boom and four outriggers are fully extended and the boom angle is set at 25°. The resulting outrigger forces are symmetrical to the longitudinal axis of the mobile crane carrier with the boom located on the front, as shown in Fig. 4. The upper bounds of outrigger forces on the front pair of outriggers gradually increase to resist overturning when the load lifted is increased incrementally. The upper bounds of outrigger forces on the rear pair of outriggers are inversely correlated with the lifted load and, therefore, reduce to zero. The progressive restriction of the feasible ranges between the upper and lower bounds abruptly diminishes when the load lifted exceeds 25 tons. In this scenario, the front outriggers carry the total weight of the crane and load, and the rear outriggers may lift off the support surface. The maximum outrigger force is approximately 23.5 tons. The boom configuration can cause the crane to tip over in the forward direction when the load lifted exceeds the tipping load $F_{\text{load,tip}}$ of 25 tons.

Figure 5(a) presents a polar plot of the moment index S_{moment} versus rotation angle θ of the upper rotary crane body when the crane is supported on fully extended outriggers and the telescopic boom is 9.32m. The assumed lifted load is 25 tons. The radius of the polar diagram is proportional to the value of moment index S_{moment} , and curves are graphed at the boom angles ϕ of 0°, 20°, 30°, and 40°, respectively. The reduction in the boom angle ϕ is strongly correlated with the fact that lowering the main boom increases the moment index S_{moment} . The crane loses stability when the moment index S_{moment} lies outside the unity circle. The moment index is relatively larger near the rotation angles θ of 0°, 90°, 180°, and 270° than

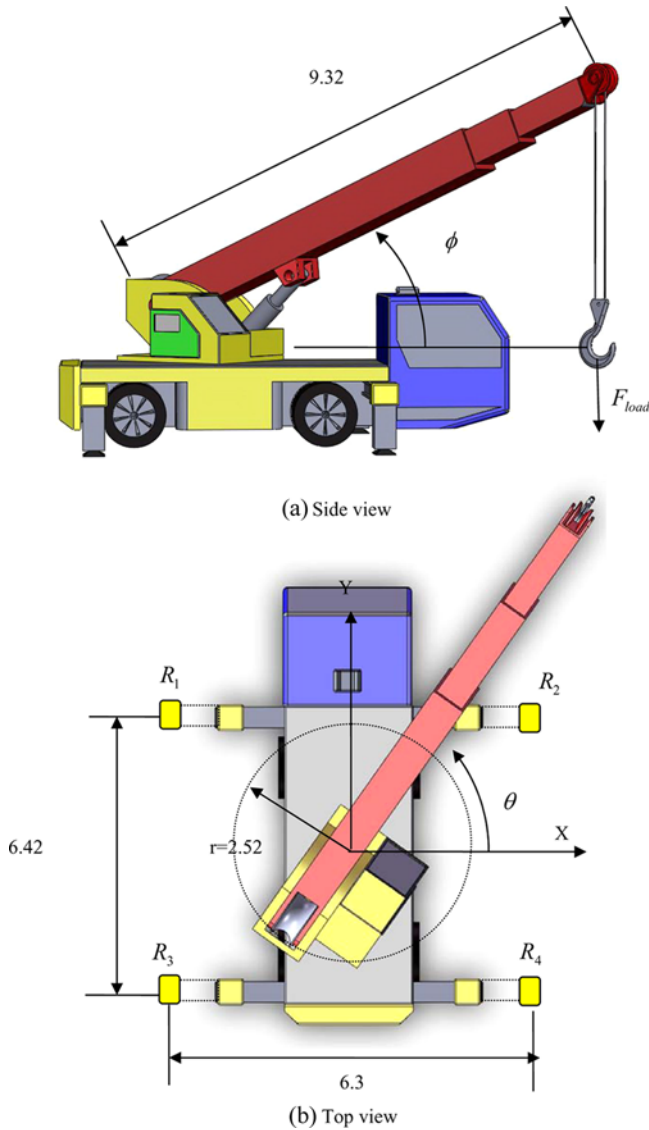


Figure 3 A mobile crane equipped with four outriggers.

that near the rotation angles θ of 45° , 135° , 225° , and 315° . Figure 5(b) presents the polar plot of force index S_{force} versus rotation angle θ . As operating a boom at an angle $<20^\circ$ results in unstable conditions in some rotation angles, which indicates that no solutions exist for maximum allowable outrigger forces, and the force index S_{force} is unavailable (Fig. 5(a)). To determine force index S_{force} for crane functions equally with full 360° rotation, the boom angle ϕ is lifted up at 30° , 40° , 50° , and 60° . The force index is large near rotation angles θ of 45° , 135° , 225° , and 315° , where the boom positions are toward the four extended outrigger locations. One way of

Table 1 Numerical data of the mobile crane equipped with four outriggers

Nomenclature	Representation	Numerical data
F_{weight}	Weight of the crane	18.08 (tons)
F_{pb1}	Weight of the first segment of boom	1.37 (tons)
F_{pb2}	Weight of the second segment of boom	1.03 (tons)
F_{pb3}	Weight of the third segment of boom	0.76 (tons)
F_{pb4}	Weight of the forth segment of boom	0.60 (tons)
R_{crit}	Maximum reaction forces of outrigger	40 (tons)
F_{eq}	Equilibrium force	0 (tones)
M_{eq}	Equilibrium moment	0
L_{length}	Length of mobile crane	6.42 (m)
L_{width}	Width of mobile crane	2.10 (m)
L_{radius}	Radius of turn table	2.52 (m)
L_{boom1}	The first segment length of boom	9.32 (m)
L_{boom2}	The second segment length of boom	7.12 (m)
L_{boom3}	The third segment length of boom	7.10 (m)
L_{boom4}	The forth segment length of boom	7.10 (m)
L_{span1}	The first lateral distance of outrigger	0.85 (m)
L_{span2}	The second lateral distance of outrigger	0.65 (m)
L_{span3}	The third lateral distance of outrigger	0.6 (m)

increasing moment stability is by rotating the boom toward the support positions of outriggers as the horizontal distance between the overturning edge and the lifted hook decreases. However, the distribution of total weight is concentrated on one outrigger, which reflects the increase in force index S_{force} . When continued operation

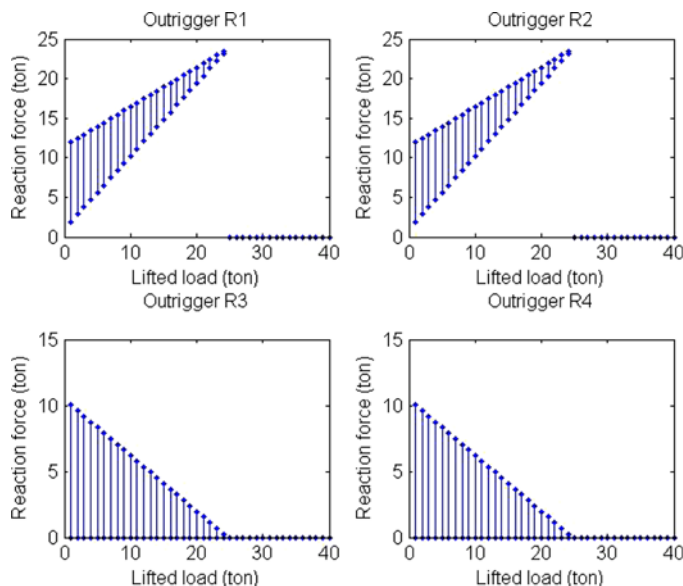


Figure 4 Four outrigger forces.

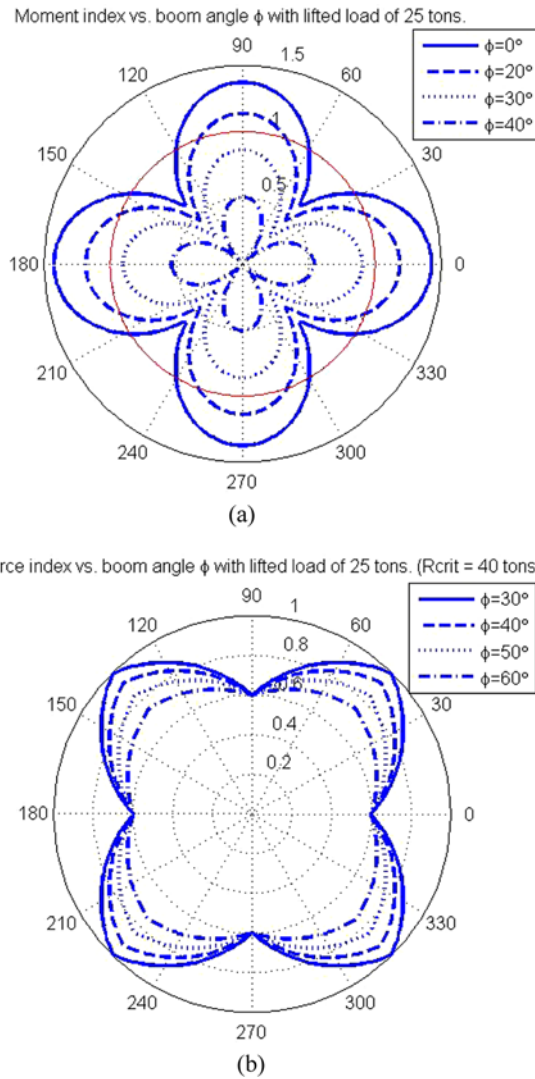


Figure 5 Moment/force indices under various boom angles for the mobile crane equipped with four outriggers.

shifts the load back to the jack, the loaded outrigger may not have been able to support the total weight, resulting in or increasing crane instability.

Figure 6 shows the set of feasible symmetrical configurations about the midline of the mobile crane with outriggers extended 70%, 80%, 90%, and 100% laterally. The telescopic boom with minimum length assumes an angle of 45° relative to horizontal. The crane is lifting 25 tons. The supplementary extensions of the suspension scaffolds generate significant additional transverse stability against overturning. The outriggers extended in the transverse direction have no effect on

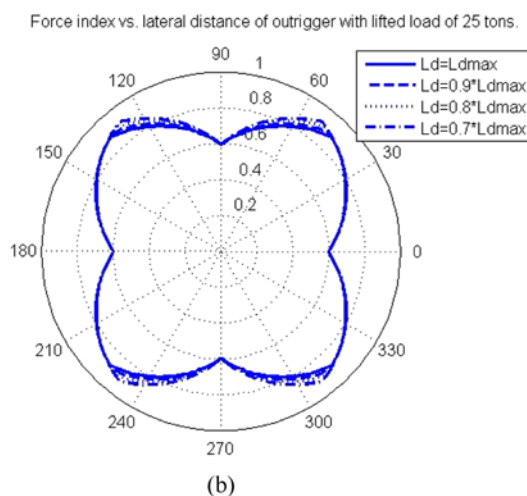
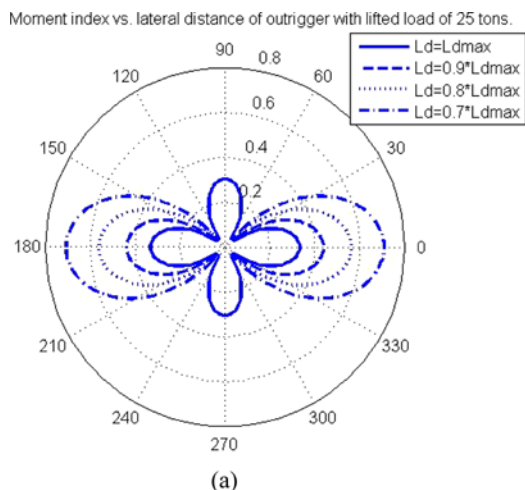
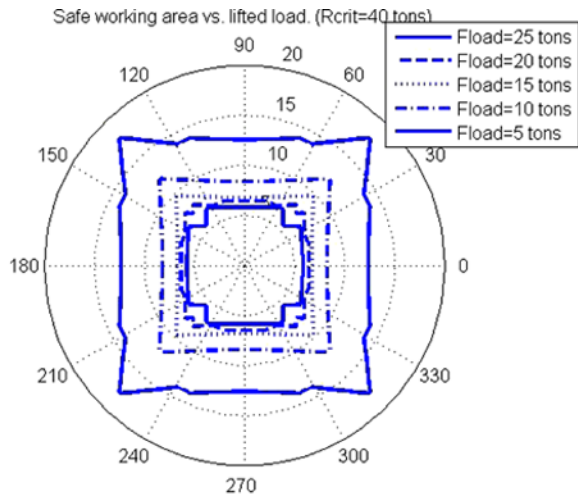


Figure 6 Moment/force indices under various lateral distances of outriggers for the mobile crane equipped with four outriggers.

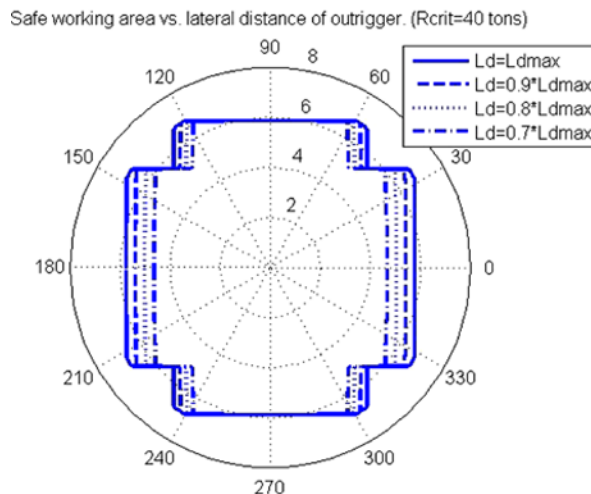
longitudinal overturning resistance when the lifting operation is in the longitudinal direction of the carrier. In the same longitudinal direction, another index for measuring outrigger forces produces a reversal effect by increasing all outriggers spreads. Force index S_{force} retains the same value, whereas rotational angle θ remains within an approximate range of -45° – 45° or 135° – 245° . A retractable outrigger is employed to increase scaffold base width and provides maximum stability when the boom points in a direction of the sliding outrigger that has the greatest extension.

The working radius, which is the horizontal distance from the crane rotational center to the boom tip can be approximately calculated using boom length, boom angle, and standard geometric principles when the boom tip deflection and fly jib offset are ignored. A safe working area is a visual representation of the orientation

angle θ of the upper rotary crane body in relation to the working radius. The crane is operated safely when a lifted load is below the safety limit at a working radius. Figure 7(a) presents simulation results for safe working areas when the mobile crane is configured to lift various loads with fully extended outriggers. The safe working areas, symmetrical about the midline of the mobile crane, are extremely similar to the convex area formed by outrigger connection lines. Since the working radius is set to account for force indices, the four corner regions of working areas are removed to prevent a heavy load from being concentrated on a single outrigger when the



(a)



(b)

Figure 7 Safe working areas of the mobile crane equipped with four outriggers.

load lifted exceeds 20 tons. Lift capacity decreases as safe working area increases. Figure 7(b) plots safe working areas versus outrigger positions when lifting 25 tons. The outrigger transversal spreads provide an additional safe working area in the transversal direction. The safe working area along the longitudinal direction is independent of extended outriggers. The four corner regions in the rectangular safe working area are restricted as the vertical reaction force of an outrigger markedly exceeds the mechanical limited axial load R_{crit} of 40 tons.

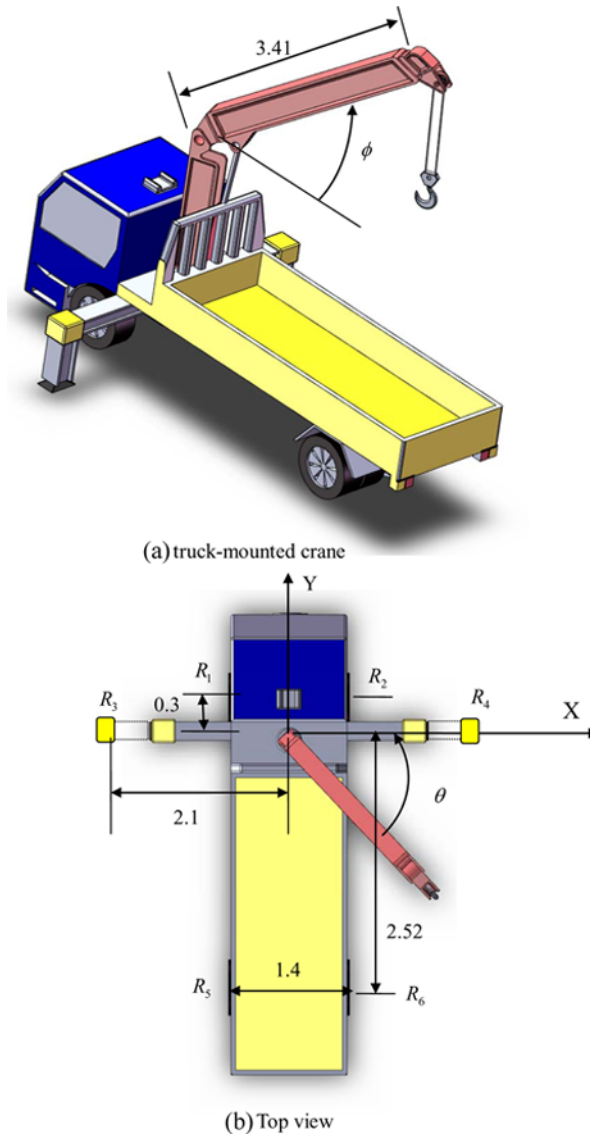


Figure 8 A truck-mounted crane with six supporting points.

Example 2: Truck-Mounted Crane with Six Supporting Points

Figure 8 presents a crane mounted directly onto a rubber-tire truck that drives around for maximum portability. A pair of outrigger assemblies stabilizes the truck-mounted crane. This crane is generally designed such that vehicle wheels provide stability with additional assistance. Table 2 summarizes the mechanical data for the following simulation.

The telescopic boom with a length of 5.5 m and a boom angle of 10° operates toward the right side of the truck. The rotation angle θ is 0° and the two outriggers are fully extended. Figure 9 shows the relationships between allowable vertical reaction forces of six support points and the external load lifted. As the load lifted increases, the upper bounds of outrigger forces on support points R_1 , R_3 , and R_5 are monotonic decreasing functions of the lifted load, and the upper bound of outrigger forces on support point R_4 is a monotonic increasing function. The upper bounds of outrigger forces on support points R_2 and R_6 decrease before increasing. When there are more than four support points, the maximum allowable outrigger forces for the support points are not monotonic functions and typically increase or decrease in only one direction as the load lifted increases. In this case, the outrigger forces of points R_1 , R_2 , R_3 , and R_5 decrease gradually and, therefore, decrease to zero. Total weight of the lifted load and crane are concentrated onto areas covered by support points R_4 and R_6 when a tipping load of 4 tons is applied. The crane loses stability and the wheels and outrigger at points R_1 , R_2 , R_3 , and R_5 lift completely off the ground. Maximum outrigger forces on support points R_4 and R_6 are about 10.0 tons and 2.9 tons, respectively.

Figure 10 presents two polar plots that visually represent the orientation of the rotary crane in relation to moment and force indices. The crane is supported on fully extended outriggers and minimum boom length is assumed. The moment index is greater than unity when the crane operates with a rotation angle θ between

Table 2 Numerical data of the truck-mounted crane with six supporting points

Nomenclature	Representation	Numerical data
F_{weight}	Weight of the truck-mounted crane	8 (tons)
F_{pb1}	Weight of the first segment of boom	0.3 (tons)
F_{pb2}	Weight of the second segment of boom	0.25 (tons)
F_{pb3}	Weight of the third segment of boom	0.23 (tons)
F_{pb4}	Weight of the fourth segment of boom	0.2 (tons)
R_{crit}	Maximum reaction forces of outrigger	10 (tons)
F_{eq}	Equilibrium force	0 (tones)
M_{eq}	Equilibrium moment	0
L_{width}	Width of the truck-mounted crane	1.4 (m)
L_{boom1}	The first segment length of boom	3.41 (m)
L_{boom2}	The second segment length of boom	2.09 (m)
L_{boom3}	The third segment length of boom	2.19 (m)
L_{boom4}	The fourth segment length of boom	2.28 (m)
L_{span1}	The first lateral distance of outrigger	0.31 (m)
L_{span2}	The second lateral distance of outrigger	0.44 (m)
L_{span3}	The third lateral distance of outrigger	0.35 (m)
L_{span4}	The fourth lateral distance of outrigger	0.3 (m)

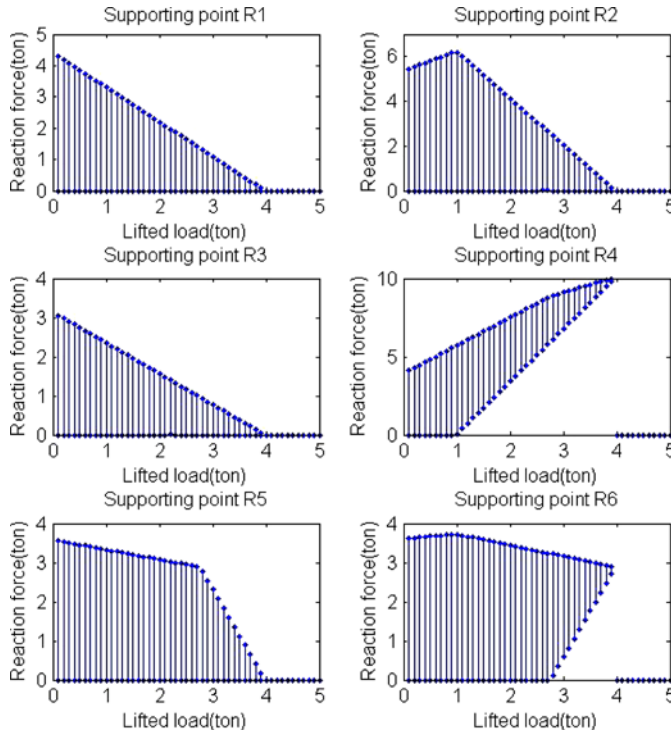


Figure 9 Allowable vertical reaction forces on the six supporting points.

50–130° and boom angle ϕ is $<50^\circ$ (Fig. 10(a)). The force index is assumed to be 0 within the unstable regions (Fig. 10(b)). An increase in the boom angle increases stability. Full orientation angles of the rotary crane body should be avoided as far as practically possible because the stability of the truck-mounted crane may be significantly reduced when a load is swung from a crane side to the front. Such movement decreases stability and markedly enhances the tendency of the crane to roll under front loading.

Figure 11 shows the set of feasible symmetrical configurations about the midline of a mobile crane. The crane is lifting 2 tons and the boom is retracted to its minimum length and the boom angle is 10° . The set of outriggers has movable lateral extensions of 70%, 80%, 90%, and 100% on the two truck sides. The moment index S_{moment} remains the same when the rotational angle θ is within an approximate range of 245–295° or 55–125°. Depending on boom position, the outriggers extended beyond the vehicle perimeter provide moment stability by simply moving the edge of overturning relatively closer to the load. Adjustable outriggers provide stability for left-rear or right-rear loading.

Figure 12 presents the safe working areas versus lifted load and outrigger lengths. The working area is restricted when the crane operates in the front area. The working radius varies markedly for rotation angles of 15°, 50°, 130°, 165°, 250°, and 290°, where direct to the positions of the six support points. Because the heavy load concentrated on a single point may reach the strength capacity

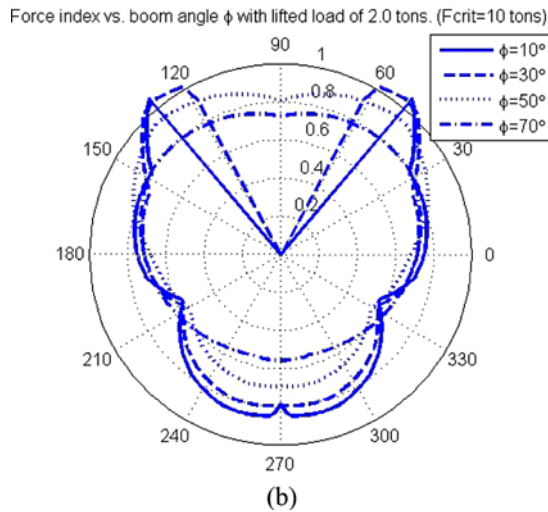
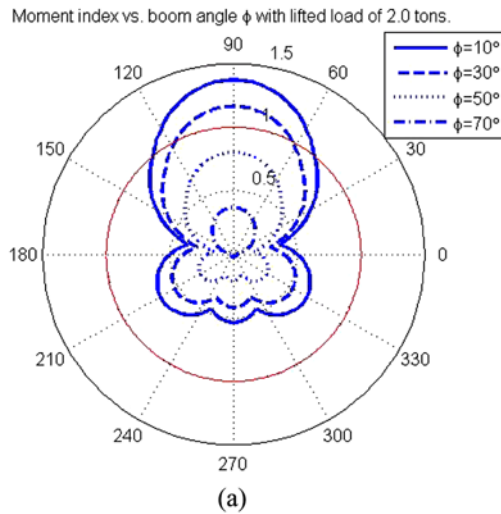


Figure 10 Moment/force indices under various boom angles for the mobile crane with six supporting points.

of an outrigger under loading, the working radius is limited. Figure 12(a) shows the resultant working radius decreases as lifted load increases. The outrigger span enlarges the safe working area, which changes based on the rotation angle of the crane at two side regions (Fig. 12(b)). As the outrigger extension increases, the safe working area increases.

SAFETY MONITORING SYSTEM

According to Fig. 13, a prototype device consisting of a main controller and four sensor modules is implemented to demonstrate the feasibility of the proposal

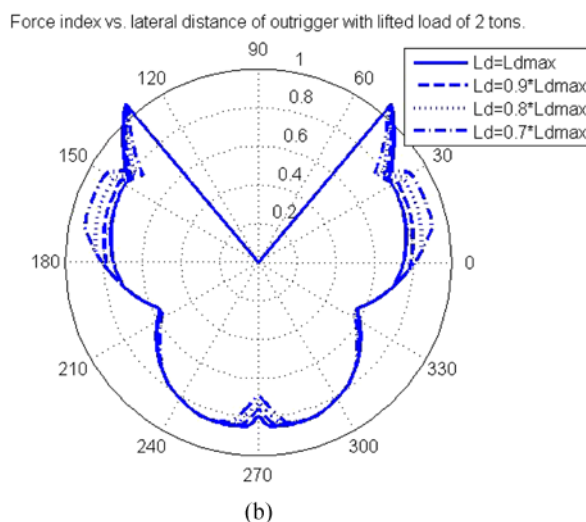
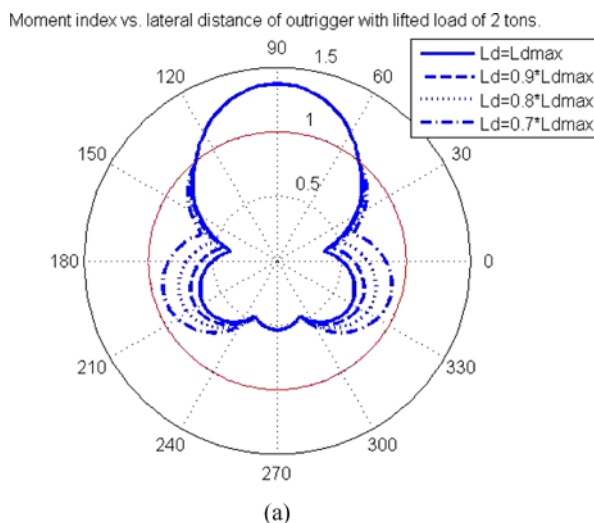


Figure 11 Moment/force indices under various lateral distances of outriggers for the mobile crane with six supporting points.

scheme in terms of automatically monitoring the online safety of a truck-mounted crane. Consisting of a strain gauge transducer, a length encoder, an inclinometer, and a shaft angle resolver with flexible brackets on laterals sides of the crane boom, the crane condition sensors provide electric signals pertaining to lifted load, boom length, boom angle, and rotational angle of the crane. A RS485 serial interface that utilizes differential and twisting signals is embedded in the sensor module. Each module located near the corresponding sensor element transports acquisition data and status events to the main controller via the industrial standard Modbus

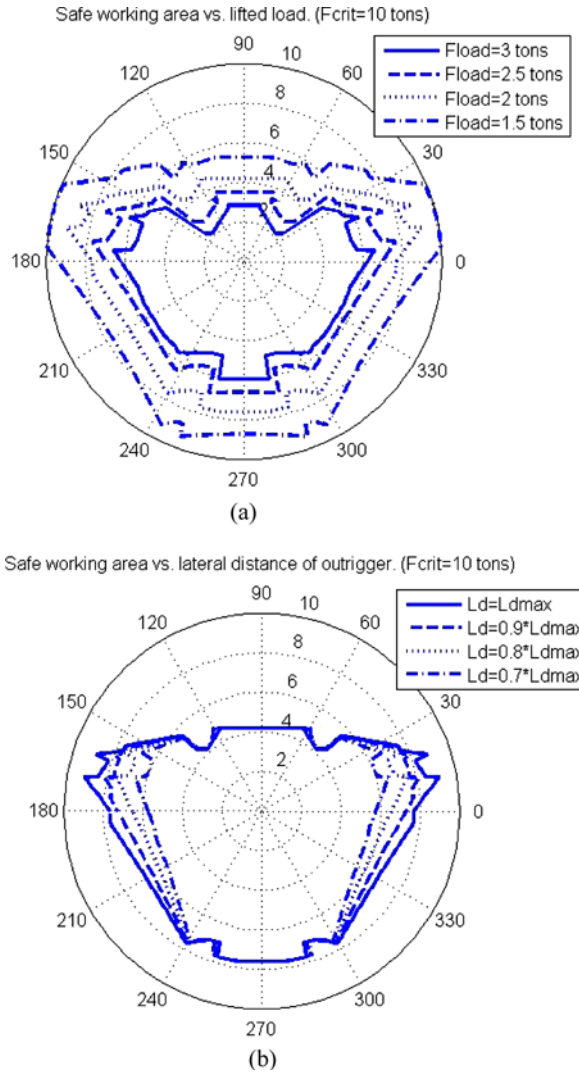


Figure 12 Safe working areas of the mobile crane with six supporting points.

RTU protocol. Simple and inexpensive to construct, the remote sensor modules are adjustable within a wide range to adhere a variety of mobile conditions.

A general purpose 8051 microcontroller is embedded in the main controller. The main controller communicates with the multiple remote sensor modules on the RS485 network. The microcontroller unit (MCU) takes user input from a six-button keypad and displays the results on a four-digit seven-segment light-emitting diode (LED) display. The main controller can provide real-time information on the lifted load, boom angle, boom length, rotation angle, and effective use of the outrigger. The solution adopted in the proposed scheme incorporates the real-time

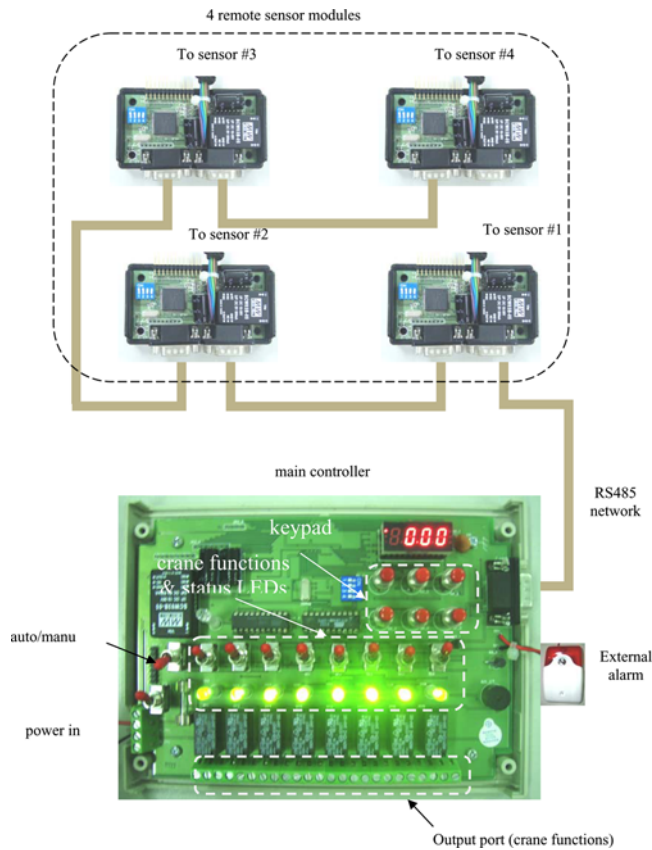


Figure 13 Antiupset monitoring system.

acquisition data pertaining to the working configuration, subsequently yielding two stability indices to ensure safe crane operations. The output signals operate visual display devices that either inform the crane operator of safe operating limits or automatically suppress certain crane functions, e.g., swinging and lifting within safe limits. The monitoring system comprises an integrated, real-time system capable of continuously monitoring, analyzing and evaluating acoustic alarm events.

COMPARISONS OF OVERTURNING MEASURES

Different measures can be applied to quantify overturning stability. A comparison of overturning moment with the stabilizing moment is a traditional measure (Queensland Government homepage, n.d.) based on which crane stability is defined as follows:

$$S_{\text{tradition}} = \frac{M_{\text{overturn}}}{M_{\text{stabilize}}} \tag{16}$$

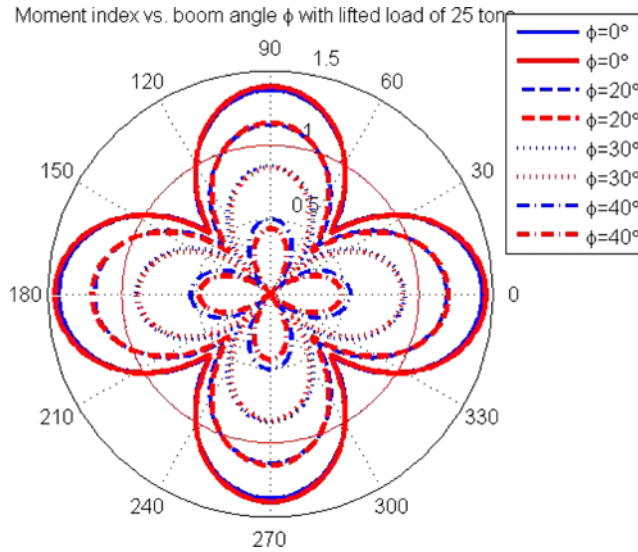


Figure 14 Comparisons between S_{moment} and $S_{\text{tradition}}$. Note that blue lines indicate S_{moment} given in this study. Red lines indicate $S_{\text{tradition}}$ (Queensland Government homepage, n.d.).

Substituting the Eqs. (11)–(14) into (16) and replacing symbol $F_{\text{load}}/F_{\text{load,tip}}$ with S_{moment} yields

$$S_{\text{tradition}} = \frac{F_{\text{load}} \cdot d_{\text{load}} + \sum_{i=1}^n F_{\text{pb}_i} \cdot d_{\text{pb}_i}}{\frac{F_{\text{load}} \cdot d_{\text{load}}}{S_{\text{moment}}} + \sum_{i=1}^n F_{\text{pb}_i} \cdot d_{\text{pb}_i}}. \quad (17)$$

These two indices, $S_{\text{tradition}}$ and S_{moment} , which are monotonic increasing functions, always increase as F_{load} increases, and are all suitable for quantifying overturning stability. Two stability indices exceeding 100% indicates that the sum of overturning moments exceeds the sum of stabilizing moments. Figure 14 shows these two indices under the same operational configuration as that in Fig. 5. The benefit of the conventional index $S_{\text{tradition}}$ is that it does not consider outrigger forces. A drawback is that the precise position of the overturning edge must be predetermined. As the gravitational center of a mobile crane does not coincide with the rotational center, determining the actual position of overturning edges is difficult. From the viewpoint of safe operation, S_{moment} , defined as the ratio of current lifted load to tipping load $F_{\text{load,tip}}$ becomes easier to recognize intuitively the safety margin than the traditional index $S_{\text{tradition}}$.

CONCLUSIONS

A mobile crane capable of lifting a predetermined load is typically equipped with an outrigger unit that comes into contact with the ground to increase lift capacity. The hosting system becomes an underdetermined system when only the static equilibrium is considered. For a crane with multiple stabilizer legs, the upper/lower bounds of outrigger forces can be obtained via two-phase simplex

algorithm. When four outriggers support a mobile crane, the minimum/maximum pruning operation that attempts to restrict the two bounds until design variables fulfill a set of inequality constraints is available to increase the computational efficiency of evaluating the allowable reaction forces of outriggers.

The moment index quantifies the tendency of tip-over behavior of a mobile crane; the force index ensures that outriggers do not fall through the pavement, sink into soft ground, or collapse. These two indices can be expressed as a function of a chassis rotational angle, boom angle, boom length, and outrigger length. Notably, simultaneously increasing the boom angle and decreasing the boom length increases stability. Additionally, outriggers decrease the overturning moment by simply moving the reference point in close proximity to the load. Lift capacities are adjusted based on boom position, in which the left/right and front/rear sides of the mobile crane are differentiated.

Importantly, this work contributes to efforts to improve stability measure. Although capable of easily determining crane stability under operating configurations, the conventional relationship between stabilizing and overturning moments does not consider outrigger reaction forces. Determining the outrigger forces is an effective means of accurately predicting the risk of overturning for a mobile crane, ultimately protecting a crane against support failure. A real-time antiupset device that monitors these two indices warns the crane operator via a signal if the load moment upsets the crane or the failure risk of the supporting surface is approached or exceeded. A practical safe working area that reflects an actual situation closely resembles the configuration of outrigger supports with cutting corners.

As is well known, a static finite element (FE) can assess precisely overturning stability due to deformation of either the crane or the outriggers that may lead to an extremely different nature of the overturning stability. Mobile crane manufacturers must analyze the shape and dimension of the mechanical parts during the design phase. However, the scheme adopted in this study is more appropriate for a microprocessor-based antiupset device that involves real-time monitoring of crane stability.

NOMENCLATURE

F_{weight}	gravitational force of upper mobile crane
F_{pb_j}	gravitational force of section j of the telescopic boom
$F_{\text{eq},x}, F_{\text{eq},y}, F_{\text{eq},z}$	three components of equilibrium force
$M_{\text{eq},x}, M_{\text{eq},y}, M_{\text{eq},z}$	three components of equilibrium moment
$R_{j,x}, R_{j,y}, R_{j,z}$	three components of reaction force of outrigger j
$R_{j,\text{max}}$	upper bound of reaction force of outrigger j
$R_{j,\text{min}}$	lower bound of reaction force of outrigger j
R_{crit}	maximum reaction force of outrigger
F_{load}	lifted load
$F_{\text{load,tip}}$	tipping load
$(x_{\text{weight}}, y_{\text{weight}})$	gravitational center of upper mobile crane
$(x_{\text{pb}_j}, y_{\text{pb}_j})$	gravitational center of section j of the telescopic boom
(x_{R_j}, y_{R_j})	center point of outrigger j

$(x_{\text{load}}, y_{\text{load}})$	center point of lifted load
θ	rotation angle of the chassis
ϕ	boom angle
S_{moment}	moment index
S_{force}	force index
$M_{\text{stabilize}}$	stabilized moment
M_{overturm}	overturning moment

APPENDIX

The following steps summarize the procedure and corresponding rationale for determining the overturning stability of a mobile crane equipped with four outriggers.

Step 1: Initial feasible range of the outrigger force $R_{4,z}$

$$R_{4,\max} = \infty \quad \text{and} \quad R_{4,\min} = 0$$

Step 2: Obtain the new feasible range of the outrigger force $R_{4,z}$ from equations in (9) and (10).

For $i = 1, 2, 3$

If $\Delta_{i,4}/\Delta_{R_1R_2R_3} > 0$ then

$$R_{4,\max} = \min \left(R_{4,\max}, \frac{Q_i}{\Delta_{i,4}} \right)$$

Else

$$R_{4,\min} = \max \left(R_{4,\min}, \frac{Q_i}{\Delta_{i,4}} \right)$$

End if

End for-loop

Step 3: An infeasible constraint implies an unstable crane; otherwise, the smaller and largest allowable values can be derived for each outrigger force using equation in (7).

If $R_{4,\max} < R_{4,\min}$ then

Print “the mobile crane is unstable”

Else

For $i = 1, 2, 3$

If $\Delta_{i,4}/\Delta_{R_1R_2R_3} > 0$ then

$$R_{i,\max} = \frac{Q_i - R_{4,\min} \cdot \Delta_{i,4}}{\Delta_{R_1R_2R_3}} \quad \text{and}$$

$$R_{i,\min} = \frac{Q_i - R_{4,\max} \cdot \Delta_{i,4}}{\Delta_{R_1R_2R_3}}$$

Else

$$R_{i,\max} = \frac{Q_i - R_{4,\max} \cdot \Delta_{i,4}}{\Delta_{R_1 R_2 R_3}} \quad \text{and}$$

$$R_{i,\min} = \frac{Q_i - R_{4,\min} \cdot \Delta_{i,4}}{\Delta_{R_1 R_2 R_3}}$$

End if

End for-loop

End if

ACKNOWLEDGMENTS

The authors would like to thank the Division of Occupational Safety, Institute of Occupational Safety and Health, Council of Labor Affairs of the Republic of China, Taiwan, for financially supporting this research under Contract No. IOSH89-S131.

REFERENCES

- Abo-Shanab, R. F., Sepehri, N. (2005). Tip-over stability of manipulator-like mobile hydraulic machines. *ASME J. Dynamic Systems, Measurement, and Control* 127(2):295–301.
- Al-lami, B. J., Benazzouz, D. (1991). Microprocessor based crane load state monitoring system. *International Conference on Control '91* 2:1183–1186.
- Aslan, S. K., Balkan, T., Ider, S. K. (1999). Tipping loads of mobile cranes with flexible booms. *Journal of Sound and Vibration* 223(4):645–657.
- Dubowsky, S., Gu, P.-Y., Deck, J. F. (1991). The dynamic analysis of flexibility in mobile robotic manipulator systems. *Proc. VIII World Congress on the Theory of Machines and Mechanisms*, 26–31 August, Prague, Czechoslovakia, pp. 1–12.
- Ghasempoor, A., Sepehri, N. (1998). A measure of stability for mobile manipulators with application to heavy-duty hydraulic machines. *ASME Journal of Dynamic Systems, Measurement, and Control* 120(3):360–370.
- Kato, Y., Ito, H. (1980). Study on static stability of a truck crane carrier. *Bulletin of the JSME – Japan Society of Mechanical Engineers* 181(23):1213–1219.
- Lim, T. H., Kim, Y. S., Choi, J. H., Lee, H. S., Yang, S. Y. (2004). Development of tipping-over rate computation system for hydraulic excavator having crane function. *Proceedings of the 8th Russian–Korean International Symposium on Science and Technology: KORUS* 3:76–79.
- McGhee, R. B., Frank, A. A. (1968). On the stability of quadruped creeping gaits. *Mathematical Biosciences* 3(3):331–351.
- Mezzuri, D. A., Klein, C. A. (1985). Automatic body regulation for maintaining stability of a legged vehicle during rough-terrain locomotion. *IEEE Journal of Robotics and Automation* 1(3):132–141.
- Mijailovic, R., Selmic, R. (2004). Influence of angular ball bearing deformation on truck-crane dynamic stability. *Mechanical Engineering* 2(1):83–93.

- Nagy, P. V., Desa, S., Whittaker, W. L. (1994). Energy-based stability measures for reliable locomotion of statically stable walkers: theory and application. *The International Journal of Robotics Research* 13(3):272–287.
- Neitzel, R. L., Seixas, N. S., Ren, K. K. (2001). A review of crane safety in the construction industry. *Applied Occupational and Environmental Hygiene* 16(12):1106–1117.
- Papadopoulos, E. G., Rey, D. A. (2000). The force-angle measure of tipover stability margin for mobile manipulators. *Vehicle System Dynamics* 33(1):29–48.
- Queensland Government homepage (n.d.). Mobile Crane Code of Practice 2006. www.deir.qld.gov.au/workplace/law/codes/mobilecrane/ (Last accessed on 27 August 2009).
- Siddall, J. N. (1972). *Analytical Decision-Making in Engineering Design*. Englewood Cliffs, NJ, USA: Prentice-Hall, Inc.
- Sugano, S., Huang, Q., Kato, I. (1993). Stability criteria in controlling mobile robotic systems. *Proceedings of the 1993 IEEE/RSJ International Conference on Intelligent Robots and Systems*, Yokohama, Japan, pp. 832–838.
- Tamate, S., Suemasa, N., Katada, T. (2005). Analysis of instability in mobile cranes due to ground penetration by outriggers. *Journal of Construction Engineering and Management – ASCE* 131(6):689–703.
- Towarek, Z. (1998). The dynamic stability of a crane standing on soil during the rotation of the boom. *International Journal of Mechanical Sciences* 40(6):557–574.
- Truninger, R. (1992). A watchdog for the overturn stability supervision of platforms. *IEEE International Conference on Systems Engineering* 139–142.
- Zhou, Z., Li, F., Huang, X. (2007). Safety monitoring method of hoisting equipment based on pressure measuring. *8th International Conference on Electronic Measurement and Instruments ICEMI '07* 2:504–507. DOI: 10.1109/ICEMI.2007.4350727